# Minimal effective Gibbs ansatz: A simple protocol for extracting an accurate thermal representation for quantum simulation

J. Cohn

*Department of Physics, Georgetown University, Washington, DC 20057, USA*
*and IBM Research Almaden, San Jose, California 95120, USA*

F. Yang

*Departments of Computer Science and Physics, University of California, Berkeley, California 94720, USA*

K. Najafi

*Department of Physics, Georgetown University, Washington, DC 20057, USA*
*and Department of Physics, Virginia Tech, Blacksburg, Virginia 24061, USA*

B. Jones

*IBM Research Almaden, San Jose, California 95120, USA*

J. K. Freericks ⬤

*Department of Physics, Georgetown University, Washington, DC 20057, USA*

Quantum Gibbs state sampling algorithms generally suffer from either scaling exponentially with system size or requiring specific knowledge of spectral properties *a priori*. These algorithms also require a large overhead of bath or scratch or ancilla qubits. We propose a method, termed the minimal effective Gibbs ansatz (MEGA), which uses a quantum computer to determine a small effective ensemble of pure states that accurately reproduce thermal averages of an objective dynamic correlation function. This technique employs properties of correlation functions that can be split into lesser and greater parts; here, we primarily focus on single-particle Green's functions and density-density correlators. When properly measured, these correlation functions provide a simple test to indicate how close a given pure state or ensemble of pure states is to providing accurate thermal expectation values. Further, we show that, when properties such as the eigenstate thermalization hypothesis hold, this approach leads to accurate results with a sparse ensemble of pure states; sometimes only one suffices. We illustrate the ansatz using exact diagonalization simulations on small clusters for the Fermi-Hubbard and Hubbard-like models. Even if the MEGA becomes as computationally complex as other Gibbs state samplers, it still gains an advantage due to its ease of implementation without any *a priori* information about the Hamiltonian and in the efficient allocation of available qubits by eliminating bath qubits and using a minimal number of ancillas.

## I. INTRODUCTION

In the mid 1990s it was shown that the time evolution of many-body quantum systems can be simulated efficiently on a quantum computer [1]. Since then much progress has been made in developing quantum algorithms for simulating these systems [2–4]. The ability to extract correlation functions, such as single-particle Green's functions which are important for understanding the bulk behavior of condensed-matter systems, has also been developed for quantum computers [5–8]. One difficulty, generally overlooked in these algorithms, is that of initial state preparation. While exploring time dynamics will eventually be a straightforward process on an ideal quantum computer, the complexity of preparing physically relevant states can be challenging for certain systems [9].

This is especially true when it comes to preparing Gibbs thermal states at low temperature. Certain algorithms are able to achieve quantum Gibbs state preparation but generally require a large overhead of ancilla or bath qubits and a long run time [10,11]. Other approaches can be more efficient, but require *a priori* knowledge about specific spectral properties such as correlation lengths or spectral gaps [12–14]. Recently, more approximate approaches to Gibbs state sampling have been explored [15–17].

Here we propose a framework termed the minimal effective Gibbs ansatz (MEGA), which uses quantum computers to construct a small set of pure states that effectively produces an accurate representation of an objective, finite-temperature, dynamic correlation function. The term "minimal," used in the framework, is not used in a mathematically rigorous sense, but

rather colloquially in the context of the framework which we present. The MEGA works with any correlation function that can be separated into lesser and greater parts. When a system is in thermal equilibrium, these functions can be Fourier transformed from the time domain to the frequency domain. Here, the fluctuation-dissipation theorem (for grand-canonical ensembles) schematically gives

$$\frac{\mathcal{F}^<(\omega)}{\mathcal{F}^>(\omega)} = -e^{-\beta(\omega-\mu)}, \tag{1}$$

for correlation functions of fermionic operators, and

$$\frac{\mathcal{B}^<(\omega)}{\mathcal{B}^>(\omega)} = e^{-\beta\omega}, \tag{2}$$

for correlation functions of bosonic operators, where $\beta$ is the inverse temperature and $\mu$ is the chemical potential. In this work, we focus on two specific types of correlation functions: single-particle Green's functions and density-density correlation functions.

The MEGA approach requires one to efficiently prepare pure states within a certain energy window, where the ensemble of pure states resembles a mixed state that is diagonal in the energy eigenbasis. Then, using well-known quantum circuits, we extract the lesser and greater parts of the Green's function with respect to each prepared pure state in the ensemble [7,8]. Using the known relation of the ratio between the lesser and greater components, given in Eqs. (1) and (2), one can classically extract the optimal $\beta$ and $\mu$ from a linear least-squares fit, whose errors serve as an indicator of how well the current ensemble approximates the corresponding exact result, calculated from the full Gibbs state.

One advantage of the MEGA lies in its simple implementation and its efficient use of qubits. If one has no prior information as to whether a minimal thermal representation of pure states may exist, one can simply implement the MEGA and test how quickly the results converge. If it does not converge well, then it would be more appropriate to use a different Gibbs state preparation or sampling algorithm. Further, we expect the MEGA to efficiently create a minimal representation in systems where the eigenstate thermalization hypothesis holds, or at temperatures where the system has a finite correlation length [13,18–21].

We aim to lay out a simple framework, in which quantum computers can efficiently extract thermal properties of many-body systems. The paper is structured as follows. In Sec. II, we briefly review single-particle Green's functions. In Sec. III, we discuss heuristic arguments that support the MEGA being an efficient method, and in Sec. IV, we present numerical simulations. Finally, in Sec. V we give our concluding remarks.

## II. SINGLE-PARTICLE GREEN'S FUNCTIONS

Single-particle Green's functions are the workhorse of many-body physics. They can be employed to determine a number of properties directly, such as the total energy, double occupancy, kinetic energy, electron filling, etc. In addition, they are required in formulating more complicated response functions like an optical conductivity or a magnetic susceptibility (when supplemented by vertex functions). Here, we also primarily focus on the lesser and greater Green's functions,
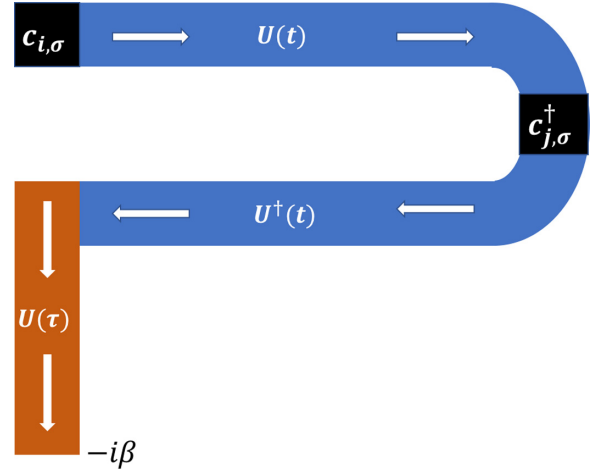


FIG. 1. The Keldysh contour for the lesser Green's function, with $t > 0$. Here, the matrix element that defines the lesser Green's functions shows that one first annihilates a particle at site $i$, then evolves the system for a time $t$, creates a particle at site $j$, evolves backwards in time again for a time $t$, and finally evolves down the imaginary axis to the desired inverse temperature $\beta$.

which can be seen as a decomposition of the retarded Green's function in the following manner:

$$G^>_{ij\sigma}(t) = -i\langle \hat{c}_{i,\sigma}(t)\hat{c}^\dagger_{j,\sigma}(0)\rangle, \tag{3}$$

$$G^<_{ij\sigma}(t) = i\langle \hat{c}^\dagger_{j,\sigma}(0)\hat{c}_{i,\sigma}(t)\rangle, \tag{4}$$

$$G^R_{ij\sigma}(t) = \Theta(t)[G^>_{ij\sigma}(t) - G^<_{ij\sigma}(t)]. \tag{5}$$

A visualization of the lesser Green's function is displayed by the Kelydsh contour in Fig. 1. Here the angle brackets represent thermal averaging with respect to the equilibrium thermal Gibbs state:

$$\rho_G(\beta) = \frac{1}{\mathcal{Z}(\beta)}e^{-\beta\hat{H}}, \tag{6}$$

where $\mathcal{Z}(\beta)$ is the partition function

$$\mathcal{Z}(\beta) = \text{Tr}\{e^{-\beta\hat{H}}\}. \tag{7}$$

The time dependence of the operators is in the Heisenberg representation. The $\hat{c}_{i,\sigma}$ ($\hat{c}^\dagger_{i,\sigma}$) operators represent the Fermionic annihilation (creation) operators at the $i$th site on a lattice for a given $z$ component of the spin, $\sigma \in \{\uparrow, \downarrow\}$.

When periodic boundary conditions are imposed on the real-space lattice, the creation and annihilation operators can also be represented in momentum space as

$$\hat{c}_{\vec{k},\sigma} = \frac{1}{\sqrt{L}}\sum_{j=1}^L \hat{c}_{j,\sigma}e^{-i\vec{k}\cdot\vec{R}_j}, \tag{8}$$

where $\vec{k}$ is a reciprocal lattice vector, $\vec{R}_j$ is the real-space position vector of the $j$th site, and $L$ is the number of lattice sites.

One can also express the Green's functions in what is known as the Lehmann representation by expanding the trace as a sum over the energy eigenstates (which satisfy $\hat{H}|E_n\rangle = E_n|E_n\rangle$) and inserting a resolution of the identity operator in

between the creation and annihilation operators. This is shown below for the lesser Green's function:

$$G^<_{ij,\sigma}(t) = \sum_n \frac{e^{-\beta E_n}}{\mathcal{Z}(\beta)} \langle E_n | \hat{c}^\dagger_{i,\sigma} e^{i\hat{H}t} \hat{c}_{j,\sigma} e^{-i\hat{H}t} | E_n \rangle \quad (9)$$

$$= \sum_n \frac{e^{-\beta E_n}}{\mathcal{Z}(\beta)} \sum_m e^{-i(E_n - E_m)t} |\langle E_n | \hat{c}^\dagger_{i,\sigma} | E_m \rangle|^2. \quad (10)$$

Fourier transforming Eq. (10) from the time domain to the frequency domain we likewise obtain

$$G^<_{ij,\sigma}(\omega) = 2\pi i \sum_n \frac{e^{-\beta E_n}}{\mathcal{Z}(\beta)} \sum_m \delta(\omega - E_n + E_m)$$

$$\times |\langle E_n | \hat{c}^\dagger_{i,\sigma} | E_m \rangle|^2. \quad (11)$$

An important physical property that we also focus on is the local density of states (per spin) given by

$$A_\sigma(\omega) = -\frac{1}{\pi} \mathrm{Im}\big[G^R_{ii,\sigma}(\omega)\big] = \frac{1}{2\pi} \mathrm{Im}[G^<_{ii,\sigma}(\omega)]. \quad (12)$$

The fluctuation-dissipation theorem for Green's functions gives

$$\frac{G^<_{ij,\sigma}(\omega)}{G^>_{ij,\sigma}(\omega)} = -e^{-\beta(\omega-\mu)}, \quad (13)$$

which can be easily derived from the grand-canonical ensemble. The formulas for the grand-canonical formalism result from shifting the Hamiltonian operator by the chemical potential multiplied by the electron number operator: $\hat{H} \to \hat{H} - \mu\hat{N}$, with $\hat{N}$ being the total particle number operator.

## III. ANALYSIS AND HEURISTICS

Here, we use heuristic arguments to analyze situations in which the MEGA is well suited, and examine its limitations. We do not give any rigorous bounds for particular Hamiltonians but rather justify the use of this approach by using physical arguments. The MEGA benefits from not needing all the resources required to prepare full Gibbs states when calculating dynamic correlation functions of a moderately sized system. We assume the system we describe corresponds to a periodic lattice that is translationally invariant, so that every site is identical.

The aim of the MEGA framework is to find a small set of pure states, $\{|\psi_i\rangle\}$, in which expectation values of a specific dynamic correlation function yield accurate approximations compared to those determined from the corresponding Gibbs state. Based on ensemble equivalence, if we sample states from a restricted energy window this microcanonical ensemble will be equivalent to any other thermodynamic ensemble in the thermodynamic limit. The MEGA also takes advantage of the inherent fluctuation theorems related to the dynamic correlation function of interest. The fluctuation theorems are used to measure how well the current set of states approximates the true thermal result. With these properties in mind we propose the MEGA as a framework to approximate finite-temperature dynamic correlation functions.

An outline of the MEGA procedure is as follows:

(1) Prepare $|\psi_i\rangle$ with $N$ electrons and within an appropriate energy window. (One has the option of additionally employing projective measurements here depending on available resources to remove states that fall outside the desired window).

(2) Repeatedly use the same state preparation procedure to measure $G^<_{ij,\sigma}(t)$ and $G^>_{ij,\sigma}(t)$ at a series of points in time. Extend the time points far enough out that the Green's function can have its tail fit to an exponential or power-law decay. (Negative times can be extracted by using the relation that the imaginary parts of the lesser and greater Green's functions are symmetric about $t = 0$ and the real parts are antisymmetric about $t = 0$).

(3) On a classical computer, perform a Fourier transform from time to frequency, approximating the real-time Green's functions by the fit tail for large enough times. Extract a least-squares fit of $\beta$ and $\mu$ from Eq. (13).

(4) If the least-squares fit lies below a given threshold, terminate the calculation. Otherwise, return to step 1, and prepare $|\psi_{i+1}\rangle$, possibly using least-squares fits of the current set of states to inform the state preparation procedure for $|\psi_{i+1}\rangle$.

Note that there is no guarantee that the MEGA will produce a sparse representation of a thermal Gibbs state, but the advantage here is that one can implement the MEGA protocol without any prior knowledge and observe how quickly the fit converges.

The precise methodology needed to create states within a given energy window will depend on the specific system as well as the hardware and resource limitations. We do not spell out a particular algorithm here, but one can choose from a variety of known methods such as adiabatic (or approximate diabatic) state preparation, the variational quantum eigensolver (VQE) [22,23], the quantum approximate optimization algorithm (QAOA) [24], quantum walk algorithms, or amplitude amplifications to construct the best approach with the given system and resource limitations [25–27]. We also note that isolating a narrow, low-energy window can still be exponentially hard for certain problems, but we expect other Gibbs state preparation algorithms to suffer here as well [9].

Users are able to tailor the MEGA based on heuristics or previously known information about the system of interest. In the strictest sense one would want detailed analysis on how the width of the energy window must scale with system size and temperature in order to produce a thermodynamic equivalent ensemble. Within the MEGA framework one may choose to construct more complicated schemes such as energy filters, construct postselection methods to restrict the energy variance, or use various time-averaging techniques to ensure stationarity.

Another property that may speed up the convergence of the MEGA is in systems where the correlations decay exponentially. In this case, we can associate a temperature-dependent correlation length $\xi(\beta)$ to the Gibbs state of a specific system. When $\xi(\beta)$ has a finite length, then sampling from a Gibbs state prepared on a system size proportional to the correlation length efficiently yields the behavior of a Gibbs state prepared on the same system in the thermodynamic limit [13,21]. One might be able to construct schemes which bound the correlation length of a given MEGA ensemble.

The ideal setting, where the MEGA would yield a sparse ensemble, is in systems where the eigenstate thermalization

hypothesis (ETH) holds. The ETH ansatz states that when a random pure state is chosen from a superposition of states originating from a narrow energy window (lying away from the edges of the spectrum of generic nonintegrable systems), then the matrix elements of typical few-body observables take the form [18]

$$\langle E_m | \hat{O} | E_n \rangle = O_{mc}(\bar{E}) \delta_{mn} + e^{-\frac{S(\bar{E})}{2}} f_O(\bar{E}, \omega) R_{mn}. \quad (14)$$

Here, $O_{mc}(\bar{E})$ is the microcanonical average of the observable $\hat{O}$ centered at the average energy $\bar{E}$ of the narrow energy window and $S(\bar{E})$ is the thermodynamic entropy defined by $\exp[S(\bar{E})] = \bar{E} \sum'_n \delta_\epsilon(\bar{E} - E_n)$, where the restricted sum is over the number of states within a smeared $\delta$ function centered at $\bar{E}$. $f_O(\bar{E}, \omega)$ is a smooth function of its arguments with $\omega = E_n - E_m$ and $R_{mn}$ is a random number with zero mean and unit variance. Here one can see that as the number of states within the energy window becomes exponentially large then the fluctuations about the microcanonical ensemble become exponentially suppressed.

An alternative way to underpin the convergence of the MEGA is via the many-body sum rules for Green's functions [28–30]. It is well known that the integral of the spectral function for fermionic systems is equal to 1. It is less known that higher moments also satisfy sum rules, which depend on parameters in the Hamiltonian and some simple thermodynamic expectation values. In the time domain, these sum rules represent the equal time Green's function values and the low-order derivatives at equal time. Hence, if the wave functions in the MEGA ensemble share the same expectation values as the Gibbs ensemble, then the first $n$ derivatives of the Green's function will be correctly reproduced by the MEGA. This implies that the MEGA will be accurate even with relatively poor choices for the wave functions if they possess the correct expectation values for reproducing the first $n$ moments. For example, the retarded local Green's function has a zeroth moment that is independent of the choice of ensemble and a first and second moment (at half filling) that depends only on the chemical potential and the interaction energy. Similarly, for the lesser Green's function, all wave functions with the right electron density have the correct zeroth moment. This general principle implies that we expect deviations between the MEGA and the Gibbs distribution to set in once the relative time is long enough. But, because these correlation functions typically decay over a finite time range, once the MEGA ensemble is large enough to properly represent this time interval, it will produce the same results as the Gibbs ensemble to a specified degree of accuracy.

One drawback of the MEGA is that we cannot dial in specific temperatures; instead one generally has approximate bounds in terms of what consists of low vs high energy for a given Hamiltonian. By preparing a state in a narrow energy window, one can then extract the effective temperature via our postprocessing procedure employing the ratio of the lesser and greater Green's functions in frequency space.

The ratio of the lesser to greater Green's functions, which we employ to test the accuracy of the MEGA for a given calculation, is derived in the grand-canonical ensemble. But the calculation procedure described above worked with a fixed filling of the electrons. This is fine for a large enough system, because the microcanonical, canonical, and grand-canonical ensembles all yield the same results [31,32]. But for finite-sized lattices, one may do better by adding states with different fermion fillings, or by weighting states in the ensemble by Boltzmann factors to improve the convergence of the MEGA. We expect the MEGA framework to become more feasible when simulating large system sizes.

One additional limitation is of numerical precision in verifying the fluctuation-dissipation theorem to extract $T$ for instances where there is a gap in the local density of states at the chemical potential. Here, we run into the problem of trying to divide two numbers that are approximately zero in the gap region.

The main limiting factor, which restricts near-term use, is the time evolution needed to extract the Green's functions. Here, we need to extract the Green's functions for many time steps extending out to at least a characteristic decay time $t = t_d$ (where the Green's function becomes vanishingly small). Optimistically, we expect the circuit depth here to scale linearly with the number of Trotter steps and hence linearly with $t_d$. The depth of each Trotter step will scale polynomially on the number of sites or orbitals. With these circuit depth requirements, we expect the MEGA to be applicable once circuit depths required for modest time evolution can be reached [33]. The MEGA approach is also limited by the complexity of preparing states within a narrow energy window, which can be difficult for certain systems, but this complexity will also limit other Gibbs state preparation algorithms as well.

The advantage of using the MEGA is in the simple implementation and the efficient use of the available qubits. Fermionic systems usually require $2L$ qubits per lattice via the Jordan-Wigner mapping to a corresponding spin Hamiltonian. There also exist parity mappings such as the Bravyi-Kitaev map that only require $L$ qubits [34]. Also, correlation functions such as single-particle Green's functions can be extracted using a single ancilla qubit [7,8]. Given this information the MEGA should require at most $2L + 1$ qubits.

## IV. NUMERICAL RESULTS

To test the validity of this approach, we focus on the repulsive one-dimensional (1D) Fermi-Hubbard model and its variants [35]. This well-known model aims to minimally account for the electron correlations by imposing an interaction that repels two electrons of opposite spin only when they are on the same site. The Hamiltonian is given by

$$\hat{H}_{\text{Hubb}} = -t \sum_{i,\sigma} (c^\dagger_{i,\sigma} c_{i+1,\sigma} + \text{H.c.}) + U \sum_i n_{i,\uparrow} n_{i,\downarrow}, \quad (15)$$

where $t$ is the strength of the electron hopping, and $U$ is the on-site repulsion term. We note the redundant use of notation here where the parameter $t$ is used to represent both the energy scale of the hopping term and time. Also the parameter $U$ is similar to the time evolution operator $\hat{U}(t)$, but they are differentiated by the operator symbol in the time-evolution operator. The context in the text should clarify the intended interpretation of these symbols.

In one dimension, the model is integrable, and can be solved by the Bethe ansatz, so it is not expected to thermalize to the proper Gibbs ensemble because of the macroscopic
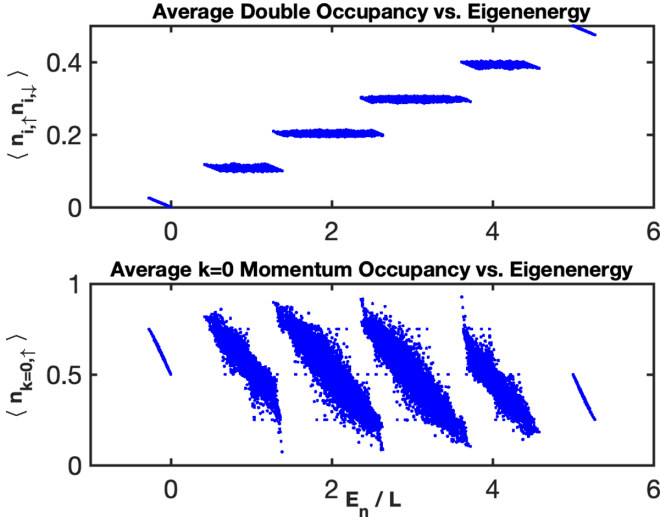
FIG. 2. Scatter plots of the average double occupancy ($\langle \hat{n}_{i,\uparrow} \hat{n}_{i,\downarrow} \rangle$) and $k = 0$ momentum occupation ($\langle \hat{n}_{k=0,\sigma} \rangle$) with respect to each energy eigenstate. One can see that when we restrict to the spin band (outlined in red) these observables are smooth monotonic decreasing functions of the eigenstate energy.

number of symmetries the model exhibits. Nevertheless, we show that adjusting certain parameters of this model allows us to predict the effectiveness of the MEGA protocol in larger nonintegrable systems. For concreteness, we also add integrability-breaking terms to the Fermi-Hubbard model and compare the performance when these terms are added. When the new terms are added the Hamiltonian becomes

$$\hat{H} = \hat{H}_{\text{Hubb}} + \hat{H}', \tag{16}$$

where

$$\hat{H}' = -t' \sum_{i,\sigma} (\hat{c}^{\dagger}_{i,\sigma} \hat{c}_{i+2,\sigma} + \text{H.c.}) + U' \sum_{i} \hat{N}_i \hat{N}_{i+1} \tag{17}$$

and $\hat{N}_i = (\hat{n}_{i,\uparrow} + \hat{n}_{i,\downarrow})$.

To begin, we examine the half-filled 1D Hubbard model with periodic boundary conditions with a large on-site interaction of $U/t = 10$, $t' = U' = 0$. This specific case is interesting because it exemplifies the ideal behavior of a system obeying the ETH. As one can see in Fig. 2, when restricted to the first energy band (spin band), both the double occupancy and the $k = 0$ momentum become smooth functions of the eigenstate energy. This is indicative of the strong ETH in the extreme sense, where every eigenstate is typical. The spectrum as a whole does not obey the ETH, so these results do not indicate physical behavior in the thermodynamic limit. Nevertheless, this behavior in the lowest band should give insight into the performance of these approximations in an ideal setting.

In general, we are more interested in simulating strongly correlated electrons rather than weakly correlated electrons, because weak correlation is amenable to many classical numerical techniques. Choosing low-energy states is relatively simple here, because at infinite interaction, there are no double occupancies at and below half filling. These states are also easy to generate on a quantum computer as product states. So, our strategy is to initialize the system in a state with no

double occupancy, ramp the state adiabatically from infinite interaction to finite interaction, and employ such a state as one of the states in the MEGA ensemble.

For these simulations, we employ exact diagonalization and use a MEGA consisting of the two Néel states, each time evolved with a time-dependent Hamiltonian. We initially set the interaction energy to $U/t = 500$, making $t$ our energy scale. We also set $\hbar = k_b = 1$. We then evolve the system with a time-dependent interaction energy that ramps from $U/t = 500$ to $U/t = 10$ given by the time evolution operator of

$$\hat{U}_{\text{prep}}(t) = \mathcal{T}\left\{ \exp\left[ -i \int_0^t dt' \hat{H}_{\text{Hubb}}(t') \right] \right\}, \tag{18}$$
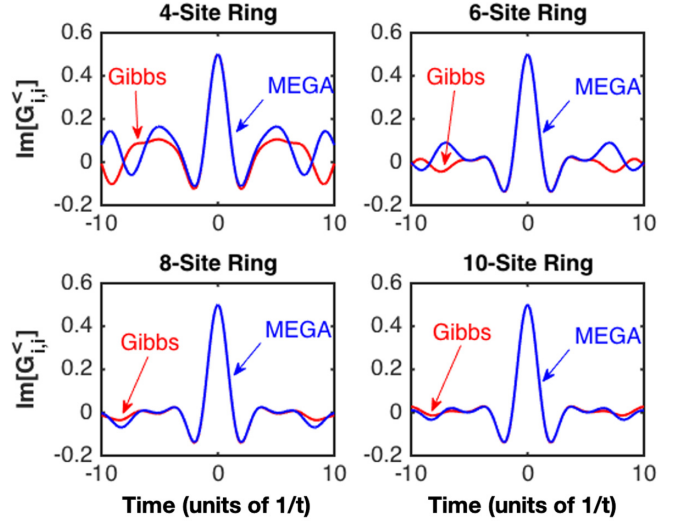


FIG. 3. Imaginary parts of the local lesser Green's function calculated with the MEGA approximation (blue curve) and with the exact Gibbs state (red curve). Here we see that the MEGA becomes accurate at longer and longer times as the system size increases.
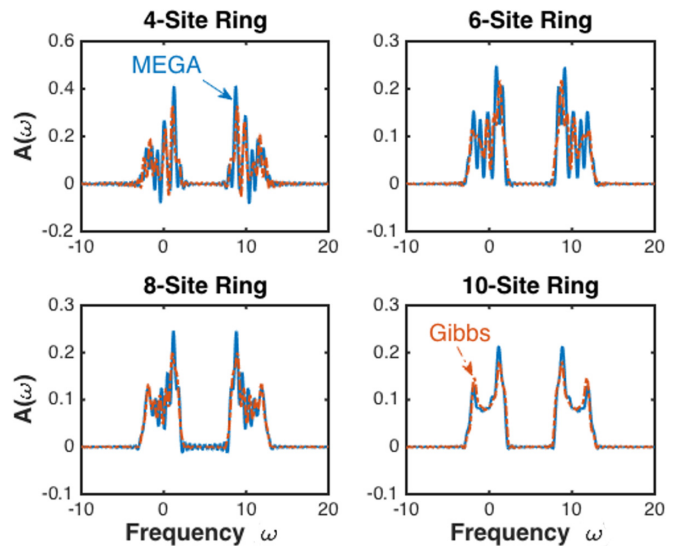


FIG. 4. Local density of states for $L = 4, 6, 8$, and 10. The gap is still identifiable for the four-site ring but each band quickly converges to the true result as the system size increases.
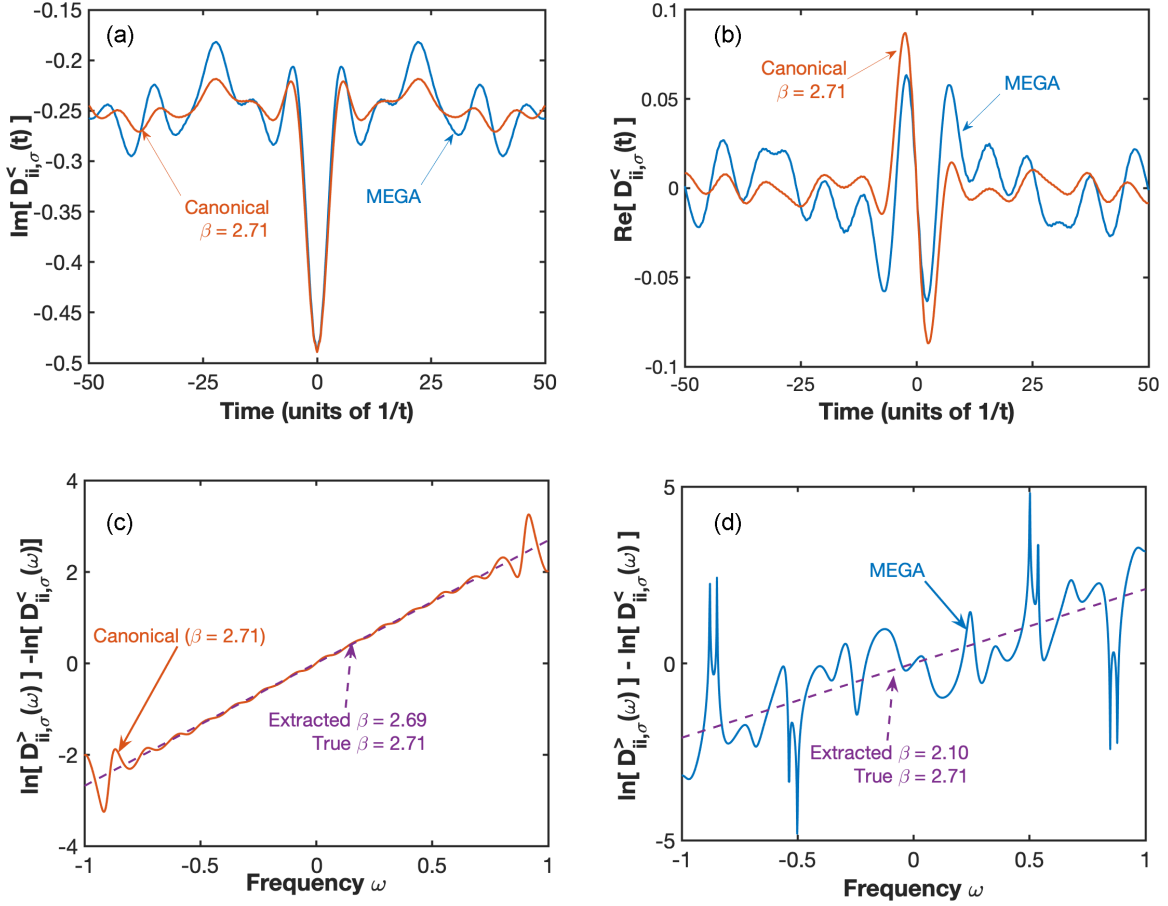
FIG. 5. Canonical Gibbs fit using the density-density correlator instead of the single-particle Green's functions for a ten-site system with $U/t = 10$. The (a) imaginary and (b) real parts of the MEGA approximation used here, $\{\hat{U}_{\text{prep}}(\tau)|\uparrow\downarrow\uparrow\cdots\rangle, \hat{U}_{\text{prep}}(\tau)|\downarrow\uparrow\downarrow,\cdots\rangle\}$, diverge from the corresponding Gibbs state at earlier times for this correlator than with single-particle Green's functions. (c) The effective temperature can be properly extracted when a large enough ensemble is used. (d) We see that the current MEGA ensemble exhibits large fluctuations and the fit for the effective temperature yields $\beta = 2.1$, where the proper Gibbs state, at the same energy of the MEGA ensemble, has an inverse temperature of $\beta = 2.7$. This indicates that the current ensemble used for the MEGA has not properly converged and will need a larger set of states.

where the time dependence of the interaction energy in the Hubbard Hamiltonian is given by $U(t) = 490e^{-t/5} + 10$. Here, our final set consists of

$$\{\hat{U}_{\text{prep}}(\tau)|\uparrow\downarrow\uparrow\cdots\rangle, \hat{U}_{\text{prep}}(\tau)|\downarrow\uparrow\downarrow,\cdots\rangle\}, \qquad (19)$$

where $\tau$ is the total ramp time. We choose to start with the simple Néel state because it is a product state in the localized basis, which would be trivial to prepare on a quantum computer. The Néel state is one of the $\binom{N}{N/2}$ degenerate product states (with the number of up spins equal to the number of down spins) in the ground state at $U = \infty$. At large but finite $U$, the Néel states will have an overlap with the ground state and a couple other low-lying energy states. When ramping down to a smaller $U$ we are guaranteed to stay in the spin band as long as we ramp slow enough. One could also ramp up from $U/t = 0$, but initializing a quantum computer to the Fermi sea is a more complicated circuit when working in real space.

The trends in Figs. 3 and 4 show what we would naively expect when examining this ideal system. The local Green's functions, when approximated by just two states, resemble

the exact results for longer and longer times as we increase the system size. The finite size effects prevent the Green's function from truly decaying to zero.

Unfortunately, the large gap in the local density of states makes extracting the effective temperature numerically unstable. We also examine a local density-density correlator defined by

$$D_{ii,\sigma}^{>}(t) = -i[\langle \hat{n}_{i,\sigma}(t)\hat{n}_{i,\sigma}(0)\rangle - \langle \hat{n}_{i,\sigma}\rangle\langle \hat{n}_{i,\sigma}\rangle], \qquad (20)$$

$$D_{ii,\sigma}^{<}(t) = -i[\langle \hat{n}_{i,\sigma}(0)\hat{n}_{i,\sigma}(t)\rangle - \langle \hat{n}_{i,\sigma}\rangle\langle \hat{n}_{i,\sigma}\rangle]. \qquad (21)$$

As shown in Fig. 5, while this correlator is capable of extracting the correct temperature with the canonical ensemble it requires a large number of states in our MEGA approach for the results to properly converge. When using our set of the two adiabatically prepared states for the MEGA approach the results diverge more quickly in the real time domain, which leads to a noisy fit when extracting the temperature. Figure 5 shows that within this MEGA ensemble there is still a large error present in the temperature extraction.
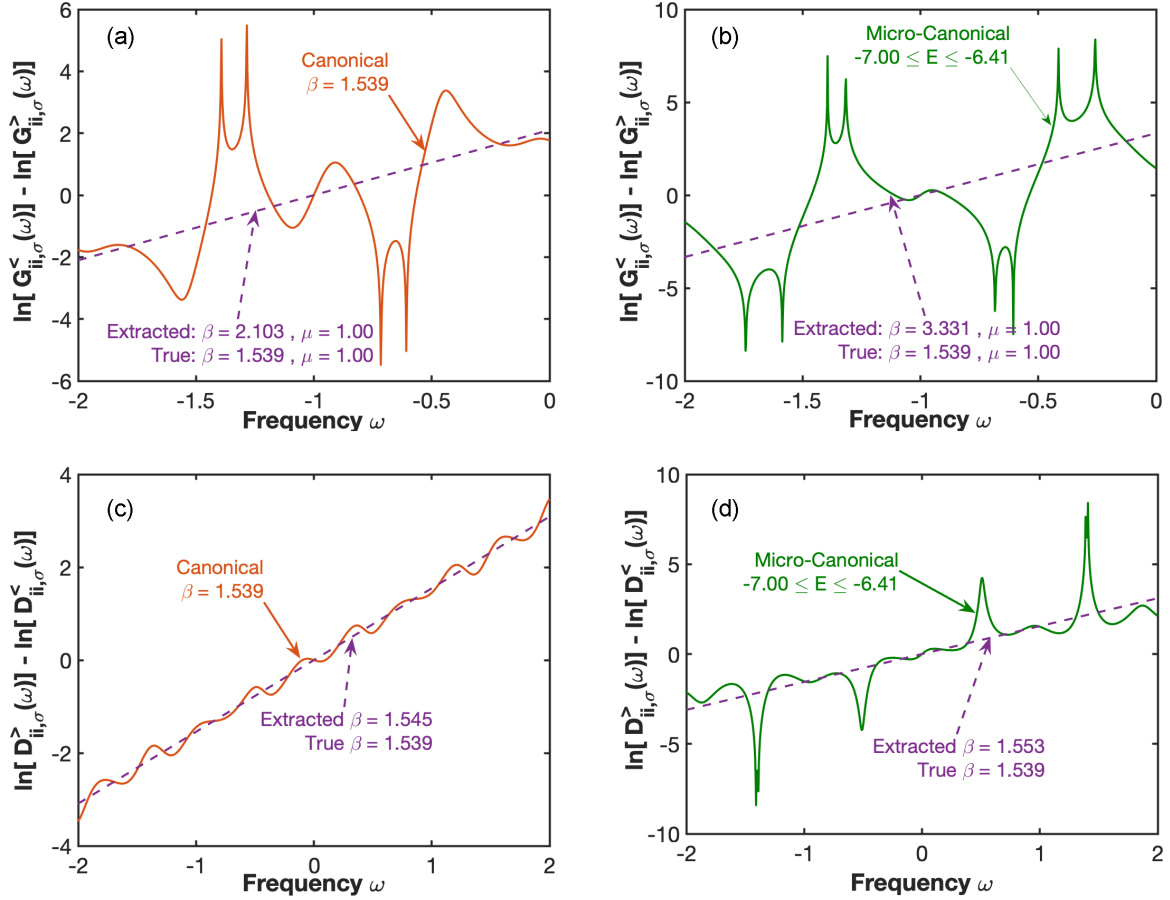
FIG. 6. Local density of states and ratio of local lesser and greater Green's functions for a ten-site system with $U/t = 2$. The systems are probed at a temperature of $T = 0.65$ and we examine the results of the canonical Gibbs state and a microcanonical window with $-7.00t \leqslant E \leqslant -6.41t$ extracted from both the local Green's function and the density-density correlator. (a, b) The local Green's functions are not able to properly extract the temperature, but do converge to the correct chemical potential. (c, d) The local density-density correlator gives a higher confidence in the temperature extraction for both the canonical and microcanonical ensembles compared to the local Green's functions.

This scenario demonstrates the difference in results for a given MEGA ensemble when examining different response functions, as well as the difference in the extracted effective temperature. Here, we see that a small MEGA ensemble accurately converges for single-particle Green's functions, but the gap in the local density of states prevents a proper test of convergence due to numerical precision errors. On the other hand, the density-density correlator is capable of accurately testing for convergence but requires the MEGA to use a larger set of states. This does bring up an important point. Different response functions may require different size ensembles in the MEGA. For response functions that can be measured with smaller ensembles, the quantum computation will be more efficient than for functions that require larger ensembles or that have large correlation lengths.

To demonstrate tests for convergence and temperature extraction with single-particle Green's functions, we work with a half-filled ten-site 1D Hubbard model with $U/t = 2$, where there is no longer a gap in the local density of states. Here the spin band is no longer separated from the rest of the spectrum, so ETH-like effects no longer hold, eliminating the ability of sparse window sampling to efficiently describe the thermal behavior. Figure 6 compares the ratio $G_{ii,\sigma}^{<}(\omega)/G_{ii,\sigma}^{>}(\omega)$ for the Gibbs state at $T = 0.65$ to a

corresponding microcanonical window. The energy window for the microcanonical ensemble is in the range $-7.00t \leqslant E \leqslant -6.41t$. We can see from Figs. 6(a) and 6(b) that the local Green's function fits do not yield the correct temperature for either the canonical or microcanonical ensembles that we have used, but the chemical potential does converge properly. The easy convergence of $\mu$ is not indicative of the Hubbard model at different fillings because this test case is performed at half filling, whose chemical potential is uniquely determined by the particle-hole symmetry. When turning to the local density-density correlator, in Figs. 6(c) and 6(d), we see a much larger confidence in the extraction of the proper temperature for each of the ensembles.

The errors that are present in these fits stem from two factors. The first is the finite energy density of the eigenvalues. Here, in the frequency domain, each of these correlators is represented by a sum over $\delta$ functions. When using small clusters there can be large fluctuations in small frequency windows due to sudden changes in spectral weight as eigenstates enter or leave a window. This can generally be alleviated by moving to larger temperature for calculations on smaller clusters. For low temperature, one would need to move to larger system sizes to extract correct results or one may be able to employ spectral broadening techniques. Once again,
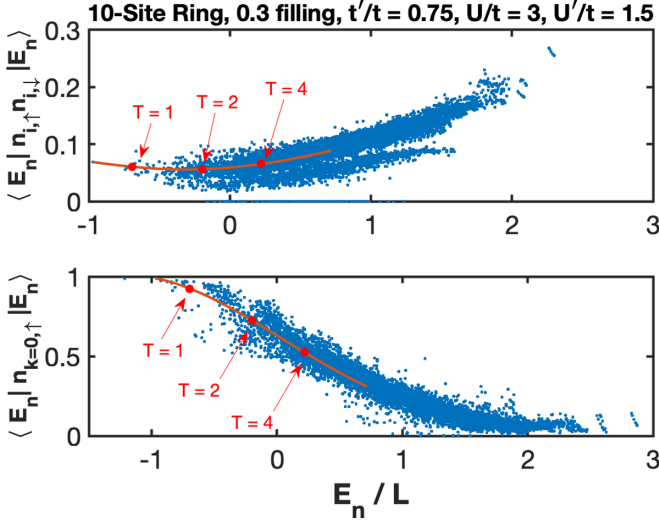
FIG. 7. Scatter plots for expectation values of double occupancy and $k = 0$ momentum occupation with respect to each energy eigenstate. Here we use a ten-site ring at 0.3 filling, with Hamiltonian parameters of $t'/t = 0.75$, $U/t = 3.0$, and $U'/t = 1.5$. As expected by the ETH ansatz, typical eigenstates in the bulk of the spectrum have small fluctuations within a narrow energy range.
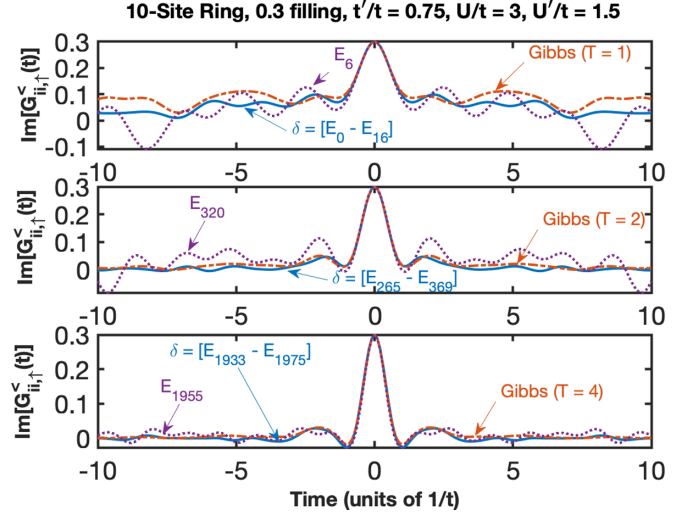


FIG. 8. Imaginary part of the local greater Green's function calculated with the microcanonical ramp state (blue curve), with the exact canonical Gibbs state (red curve), and with a single eigenstate (dotted purple curve). As one would expect from a system obeying the ETH, moving to larger temperatures allows the canonical Gibbs states to be approximated by an ensemble of a few or even a single energy eigenstate.

in situations where the correlation function is decaying in the time domain, enforcing the decay for all future times is another method that produces a continuous spectra and removes the artifacts of the $\delta$ functions.

The second driver of the error stems from situations where both lesser and greater response functions are close to zero. Here, we run into numerical precision problems from trying to divide two small numbers. In these instances, the best option is to employ a different correlator that does not suffer from both lesser and greater values being small. Convergence will also be related to the form in which the underlying operators of each correlation function spread in space and time. These are nontrivial results that normally cannot be determined before computing the results.

These results show an example of where the MEGA is able to eventually converge on a representative set of states, but the size of this set is large and would scale exponentially in system size. There is a possible fix here, as we expect this system to have a finite correlation length at finite temperature. In theory, if this finite correlation length exists, then one should be able to bound the number of representative states in the MEGA by the size of the Hilbert space on a region proportional to the given correlation length. It is still an open question as to whether an efficient state preparation scheme is feasible for the situations where the system exhibits a finite correlation length. We leave further analysis of this situation to future work.

Finally, we examine how well the MEGA would ideally work with more generic nonintegrable systems. This is achieved by working in a regime with $U/t = 3$, $U'/t = 1.5$, and $t'/t = 0.75$, where $U'$ and $t'$ are the strengths of the integrability-breaking terms defined in Eq. (21). We examine the behavior of this system again on a ten-site ring, with a filling now of $n = 0.6$.

From Fig. 7, we see that the scatter plots of the expectation values of relevant observables do not pinch down to a smooth single-valued function, as they did in the spin band above. When we are away from the edges of the spectrum, we see that most of the points clump together within a small energy range, and we see a decrease in the density if we move vertically away from this point. The ETH conjectures that these fluctuations scale inversely with the density of states, so as we move to large system sizes, we would expect the cloud to become narrower, approaching a single-valued function of the eigenstate energy. One can also see that there are nontypical states in Fig. 7 such as the states that have zero double occupancy in the middle of the spectrum. We do not know if they persist in the thermodynamic limit in the strong vs weak ETH sense [36].

For this model, we examine three areas of the energy spectrum corresponding to temperatures of $T = 1.0$, 2.0, and 4.0. For each temperature, Fig. 8 shows plots of $\text{Im}[G_{ii,\uparrow}^<(t)]$ calculated with respect to the canonical Gibbs state, a microcanonical window, and a single eigenstate, where each gives the same average energy. At $T = 1$ we can see from Fig. 7 that the energy eigenstates are sparsely populated in this regime. As a result both the microcanonical and single eigenstate Green's functions have trouble converging for times past $t \approx 1$. As we move to a temperature of $T = 2.0$ the spectrum has now become a little bit more dense. As a result the microcanonical ensemble with a large enough energy window converges rather well, and the single eigenstate holds for a slightly longer period of time before deviating from the canonical Gibbs state result. When we reach a temperature of $T = 4$ the spectrum has become rather dense. Here, a smaller microcanonical ensemble converges even better than at $T = 2$, even with a smaller number of eigenstates in its energy window, and even a single eigenstate has converged
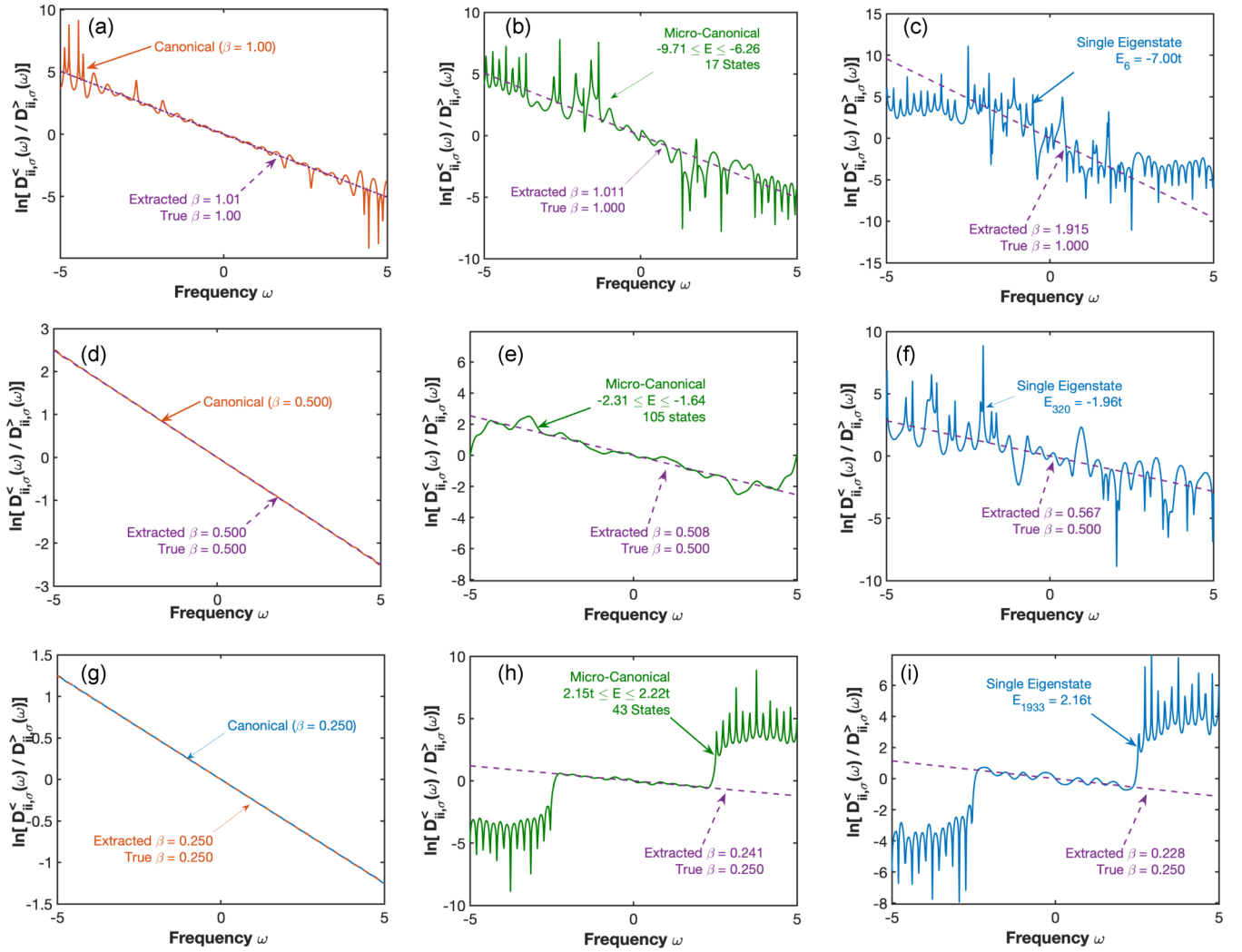
FIG. 9. Least-squares temperature fits, using the local density-density correlator, of a ten-site ring at 3/10 filling with $t'/t = 0.75$, $U'/t = 1.5$, and $U/t = 3$. The least-squares temperature fits are extracted using canonical, microcanonical, and single eigenstate ensembles which correspond to $T = 1.0$, 2.0, and 3.0. (a) For $T = 1.0$, the canonical ensemble fit is able to extract the proper temperature, but the fit is slightly noisy. (b), (c) When using a microcanonical or single eigenstate ensemble, we see that the fit becomes noisy and less accurate as we reduce the number of states used in an ideal MEGA ensemble. (d)–(f) Examining the same ensembles at $T = 2.0$ shows that the spectral weight for the canonical ensemble is large enough for the fit to be ideal, and the microcanonical and single eigenstate ensembles start to become more viable options for a sparse MEGA approximation. (g)–(i) At $T = 4.0$, we see that both a small microcanonical energy window and a single eigenstate generate relatively accurate results.

rather well for late times. The better convergence at larger temperature is what is expected from the ETH ansatz, as the entropy and density of states is much larger at higher temperatures.

Further, we continue with using the density-density correlator to examine temperature convergence as shown in Fig. 9. For the canonical ensemble we see in Fig. 9(a) that at low temperature the fit is slightly noisy, due to the low spectral density in this small cluster. We would expect the curve to smooth out as the system size increases. This sets a lower bound on the confidence level of temperature extraction in this energy range. We see that in Figs. 9(b) and 9(c), temperature extraction becomes less reliable as we reduce the number of energy eigenstates used in each ensemble. As we move to a larger temperature regime the fits become more accurate. Figures 9(d) and 9(g) show that temperature extraction for

the canonical ensemble becomes accurate at temperatures of $T = 2.0$ and $T = 4.0$. We also see that the energy window for the microcanonical ensemble can be narrowed as the temperature increases, where Fig. 9(e) uses 105 eigenstates at $T = 2.0$ and Fig. 9(h) uses 43 eigenstates and has a more accurate temperature fit. The same trend continues when trying to extract an effective temperature with a single eigenstate. Figure 9(i) shows that a single eigenstate corresponding to $T = 4.0$ begins to yield a close approximation to the actual temperature. Again, as the system size is increased, we expect that the minimum extractable temperature for each of these ensembles should reduce as well.

These results demonstrate the potential effectiveness of the MEGA in nonintegrable systems. Here, the number of states needed in a MEGA ensemble is inversely proportional to both the size of the system and the temperature.

We see that at large enough temperature or system size a MEGA ensemble of even a single eigenstate can reproduce proper thermal properties, as one would expect from the ETH framework.

There is an ultimate lower bound on the temperature extraction the MEGA is able to achieve for generic nonintegrable systems, as ETH is restricted to eigenstates that have a finite energy density. Most physical systems have either finite energy gaps or algebraically decaying energy gaps as a function of system size. This leads to a zero energy density in the large-system limit, effectively allowing large fluctuations in the matrix elements of physical observables of relevant energy eigenstates in this temperature regime. The low-temperature bound here may again potentially be alleviated if this system exhibits a finite correlation length as previously discussed. It is also possible that efficient state preparation, in this low-energy state space, can be achieved through the use of various tensor network states.

## V. CONCLUSIONS

We have outlined the MEGA protocol as a technique to examine the thermal properties of typical observables on quantum computers, and demonstrated its viability using exact diagonalization on small clusters. The advantages of the MEGA are in its simplicity to implement and the efficient use of available qubits. While the MEGA does not allow one to initially dial in a specific temperature, with an initial guess of a single of set of pure states, one can extract the effective temperature of the system that is represented by those states. Usually one has a rough idea as to within what energy range a typical state lies for what qualifies as low energy. When it is not known *a priori* whether the MEGA can be employed with a small finite set of states one can simply implement the MEGA protocol and examine how quickly $\beta$ and $\mu$ converge. We also showed numerically how systems that obey the ETH are well suited for the MEGA, in the appropriate temperature regimes and system sizes.

The efficiency of MEGA is still limited by system size here as the state preparation procedures and time evolution will scale polynomially with system size. Future work may include examining different types of correlators and possibly identifying specific properties in the feedback process to inform what the next ideal state should be to ensure faster convergence. While the MEGA is not well suited for current quantum hardware, it may be implemented on next generation or "near-term" machines once they are capable of handling the circuit depths required for modest time evolution.

## ACKNOWLEDGMENTS

[1] D. S. Abrams and S. Lloyd, Phys. Rev. Lett. **79**, 2586 (1997).

[2] D. Aharonov and A. Ta-Shma, in *Proceedings of the 35th Annual ACM Symposium on the Theory of Computing* (ACM, New York, 2003), pp. 20–29.

[3] D. W. Berry, G. Ahokas, R. Cleve, and B. C. Sanders, Commun. Math. Phys. **270**, 359 (2007).

[4] D. W. Berry, A. M. Childs, R. Cleve, R. Kothari, and R. D. Somma, Phys. Rev. Lett. **114**, 090502 (2015).

[5] G. Ortiz, J. E. Gubernatis, E. Knill, and R. Laflamme, Phys. Rev. A **64**, 022319 (2001).

[6] D. Wecker, M. B. Hastings, N. Wiebe, B. K. Clark, C. Nayak, and M. Troyer, Phys. Rev. A **92**, 062318 (2015).

[7] J. M. Kreula, L. García-Álvarez, L. Lamata, S. R. Clark, E. Solano, and D. Jaksch, EPJ Quantum Technol. **3**, 11 (2016).

[8] B. Bauer, D. Wecker, A. J. Millis, M. B. Hastings, and M. Troyer, Phys. Rev. X **6**, 031045 (2016).

[9] J. Kempe, A. Kitaev, and O. Regev, SIAM J. Comput. **35**, 1070 (2006).

[10] A. Riera, C. Gogolin, and J. Eisert, Phys. Rev. Lett. **108**, 080402 (2012).

[11] D. Poulin and P. Wocjan, Phys. Rev. Lett. **103**, 220502 (2009).

[12] M.-H. Yung and A. Aspuru-Guzik, Proc. Natl. Acad. Sci. USA **109**, 754 (2012).

[13] F. G. Brandão and M. J. Kastoryano, Commun. Math. Phys. **365**, 1 (2019).

[14] J. Van Apeldoorn, A. Gilyén, S. Gribling, and R. de Wolf, in *Proceedings of the IEEE 58th Annual Symposium on Foundations of Computer Science (FOCS)* (IEEE, New York, 2017), pp. 403–414.

[15] S. Endo, T. Jones, S. McArdle, X. Yuan, and S. Benjamin, Phys. Rev. A **99**, 062304 (2019).

[16] J. Martyn and B. Swingle, Phys. Rev. A **100**, 032107 (2019).

[17] M. Motta, C. Sun, A. T. K. Tan, M. J. Rourke, E. Ye, A. J. Minnich, F. G. Brandao, and G. K. Chan, Nat. Phys. **16**, 205 (2020).

[18] M. Srednicki, Phys. Rev. E **50**, 888 (1994).

[19] L. D'Alessio, Y. Kafri, A. Polkovnikov, and M. Rigol, Adv. Phys. **65**, 239 (2016).

[20] J. M. Deutsch, Rep. Prog. Phys. **81**, 082001 (2018).

[21] M. Kliesch, C. Gogolin, M. J. Kastoryano, A. Riera, and J. Eisert, Phys. Rev. X **4**, 031019 (2014).

[22] A. Peruzzo, J. McClean, P. Shadbolt, M.-H. Yung, X.-Q. Zhou, P. J. Love, A. Aspuru-Guzik, and J. L. O'brien, Nat. Commun. **5**, 4213 (2014).

[23] J. R. McClean, J. Romero, R. Babbush, and A. Aspuru-Guzik, New J. Phys. **18**, 023023 (2016).

[24] E. Farhi, J. Goldstone, and S. Gutmann, arXiv:1411.4028.

[25] N. Shenvi, J. Kempe, and K. Birgitta Whaley, Phys. Rev. A **67**, 052307 (2003).

[26] G. Brassard, P. Hoyer, M. Mosca, and A. Tapp, Contemp. Math. **305**, 53 (2002).

[27] D. Poulin, A. Kitaev, D. S. Steiger, M. B. Hastings, and M. Troyer, Phys. Rev. Lett. **121**, 010501 (2018).

[28] V. M. Turkowski and J. K. Freericks, Phys. Rev. B **73**, 075108 (2006).

[29] V. Turkowski and J. K. Freericks, Phys. Rev. B **77**, 205102 (2008).

[30] J. K. Freericks and V. Turkowski, Phys. Rev. B **80**, 115119 (2009).

[31] F. G. Brandao and M. Cramer, arXiv:1502.03263.

[32] H. Tasaki, J. Stat. Phys. **163**, 937 (2016).

[33] J. Haah, M. B. Hastings, R. Kothari, and G. H. Low, in *Proceedings of the 2018 IEEE 59th Annual Symposium on Foundations of Computer Science (FOCS)* (IEEE, 2018), pp. 350–360.

[34] S. B. Bravyi and A. Y. Kitaev, Ann. Phys. (New York) **298**, 210 (2002).

[35] J. Hubbard, Proc. R. Soc. London A **276**, 238 (1963).

[36] H. Kim, T. N. Ikeda, and D. A. Huse, Phys. Rev. E **90**, 052105 (2014).